Enhanced Peptide Nucleic Acid Binding to Supercoiled DNA: Possible Implications for DNA "Breathing" Dynamics†

Thomas Bentin and Peter E. Nielsen*

Center for Biomolecular Recognition, Department of Medical Biochemistry and Genetics, Biochemistry Laboratory B, The Panum Institute, Blegdamsvej 3 C, DK-2200 N Copenhagen, Denmark

Received February 22, 1996; Revised Manuscript Received May 2, 1996⊗

ABSTRACT: The influence of DNA topology on peptide nucleic acid (PNA) binding was studied. Formation of sequence-specific PNA_2/dsDNA (double-stranded DNA) complexes was monitored by a potassium permanganate probing/primer extension assay. At low ionic strengths, the binding of PNA was 2−3 times more efficient with supercoiled than with linear DNA. In the presence of 140 mM KCl, the PNA binding rate was reduced but, notably, highly dependent on template topology. Negative supercoiling (mean superhelix density, $\sigma \approx -0.051$) increased the rate of binding by 2 orders of magnitude compared to that of relaxed DNA. The pseudo-first-order rate constant [$k_\psi(\sigma)$] obeys an exponential function, $k_\psi(\sigma) = k_{\psi\mathrm{lin}}e^{-\sigma\delta}$, where δ is a constant of 105 and $k_{\psi\mathrm{lin}}$ is the rate of PNA binding to linear DNA ($\sigma = 0$). The activation energy [Ea(σ)] was determined as ≈93 and ≈48 kJ mol^{-1} for PNA binding to linear and supercoiled DNA, respectively. The results are discussed in relation to the possible future use of PNA as an antigene agent and in the framework of DNA "breathing" dynamics.

Synthetic molecules which bind sequence-specifically and with high affinity to double-stranded DNA (dsDNA)[1] may provide a way for modulating gene expression [reviewed by Maher (1992) and Hélène (1991)]. One such agent, peptide nucleic acid (PNA), was previously shown to arrest transcription *in vitro* through blockage of RNA polymerase elongation (Hanvey et al., 1992; Nielsen et al., 1994a; Peffer et al., 1993), by PNA_2/dsDNA strand invasion complexes bound to the template strand (Nielsen et al., 1994a).

PNA_2/dsDNA strand invasion complexes are formed sequence-specifically with homopurine stretches and are remarkably stable. One PNA strand binds *via* Watson−Crick hydrogen bonds, while the other forms Hoogsten bonds (Nielsen et al., 1994b). Consequently, the noncomplementary DNA strand is displaced, virtually in a single-stranded conformation (Nielsen et al., 1991, 1994b). Binding and discrimination is kinetically controlled (Demidov et al., 1995).

An apparent sensitivity of PNA strand invasion in double-stranded DNA toward moderate concentrations of salt (40−100 mM NaCl) seemed to compromise the use of PNA for antigene strategies *in vivo* (Hanvey et al., 1992; Nielsen et al., 1993, 1994b; Peffer et al., 1993). However, once formed, the PNA_2/dsDNA complex remains stable, at least up to 500 mM NaCl (Cherny et al., 1993), and thus, molecular biology applications have been developed (Demidov et al., 1993, 1994; Nielsen et al., 1993; Ørum et al., 1993).

Since PNA binding to double-stranded DNA results in DNA unwinding (Cherny et al., 1993), we speculated that binding of PNA is influenced by the substrate DNA topology. Here we show that binding of PNA to double-stranded DNA at physiologically relevant salt concentrations (140 mM KCl) is much more salt tolerant if the substrate DNA is negatively supercoiled rather than relaxed. Furthermore, the correlation between superhelical density and the rate of PNA strand invasion is established, and the activation energy for PNA strand invasion is determined.

MATERIALS AND METHODS

Topological Parameters. The linking difference (ΔLk) was used as a descriptor of supercoiling:

$$\Delta\mathrm{Lk} = \mathrm{Lk} - \mathrm{Lk}_0 \tag{1}$$

where Lk is the linking number of the topoisomer in question and Lk_0 is the linking number of a planar relaxed circle (Wr = 0). $Lk_0 = N/h_0$, where N is the number of base pairs in the circle (2698) and h_0 is the helical periodicity (10.5) (Wang, 1979) in a relaxed molecule. Conventionally, the chain length independent quantity superhelix density (σ) is used [reviewed by Vologodskii and Cozzarelli (1994)]:

$$\sigma = \frac{\Delta\mathrm{Lk}}{\mathrm{Lk}_0} \tag{2}$$

PNA. The bis-PNAs, PNA 575 [H-$(Lys)_4$-TTJTTJTTTT-$(eg)_3$-TTTTCTTCTT-Lys-NH_2] and PNA 655 [H-$(Lys)_3$-TTJTTJTTTT-$(eg)_3$-TTTTCTTCTT-Lys-NH_2] [J = pseudoisocytosine (Egholm et al., 1995); eg = 8-amino-3,6-dioxaoctanoic acid] were synthesized as described (Christensen et al., 1995; Egholm et al., 1995). PNA 575 and PNA 655 were chosen since it was found that inclusion of lysine residues (which are positively charged at pH 7.6) in bis-PNAs greatly enhances the affinity of PNA for double-stranded DNA at elevated ionic strengths (100 mM NaCl) (Griffith et al., 1995; P. E. Nielsen, unpublished experiments). PNA concentrations were determined spectrophotometrically using molar extinction coefficients for the

† This work was supported by the Danish National Research Foundation and the Novo Nordisk Corporation.

* Author to whom correspondence should be addressed.

⊗ Abstract published in *Advance ACS Abstracts,* June 15, 1996.

[1] Abbreviations: PNA, peptide nucleic acid; dsDNA, double-stranded DNA.

S0006-2960(96)00436-9 CCC: $12.00

corresponding deoxyribonucleotides: $\epsilon_{260} = 8800\ M^{-1}\ cm^{-1}$ (T) and 7300 $M^{-1}\ cm^{-1}$ (C).

Plasmid DNA. All DNA manipulations were done using standard methods (Sambrook et al., 1989). The pA8G2 plasmid was made by cloning of the oligonucleotides (5′-GTTTTCTTCTTCTGCA/5′- GAAGAAGAAAACTGCA) into the *Pst*I site of pUC19 (Nielsen et al., 1993). Propagation of pA8G2 was accomplished in *Escherichia coli* strain XL1-Blue (Stratagene). The DNA was purified using CsCl gradients followed by 1-butanol extraction. After ethanol precipitation, the DNA was dialyzed twice against 10 mM Tris-HCl and 1 mM EDTA at pH 7.6 and 4 °C for 24 h and stored in aliquots at −80 °C . Using a combination of two- [reviewed by Bowater et al. (1992)] and one-dimensional gel electrophoresis followed by quantification using scanning densitometry, we determined the mean superhelix density $\sigma \approx -0.051$ for native supercoiled pA8G2, prepared under these conditions.

PNA Binding. The plasmid DNA, pA8G2 (50 ng), was incubated in a total volume of 10−20 μL with the desired concentration of PNA at 37 °C for the indicated period of time in a buffer containing 10 mM Tris-HCl and 1 mM EDTA at pH 7.6 and other cations as denoted.

Permanganate Probing. The samples were made 1 mM in $KMnO_4$ and allowed to react for 15 s. The reactions were stopped by adding sodium acetate (pH 9.0) and 2-mercaptoethanol to final concentrations of 0.5 and 0.3 M, respectively. Following ethanol precipitation, the samples were treated with 100 μL of 10% piperidine (90 °C, 20 min), lyophilized, and prepared for primer extension by resuspension in 10 mM Tris-HCl and 1 mM EDTA at pH 7.6.

Primer Extension. The primer extension reactions were carried out in a solution containing 0.25 mM each of dGTP, dATP, dTTP, and dCTP, 20 mM Tris-HCl (pH 8.4), 5 mM $MgCl_2$, and 50 mM KCl in a final volume of 100 μL. The 5′-labeled primer (5′-AACAGCTATGACCATG) was prepared by incubating 40 pmol of oligonucleotide with 1.5 MBq [γ-^{32}P]ATP and 20 units of phage T4 polynucleotide kinase as described (Sambrook et al., 1989). To each primer extension sample was added 0.5−1 pmol of primer. The reactions were initiated by the addition of 1 unit of *Taq* polymerase. The primer extension program consisted of denaturation (94 °C, 4 min in cycle 1, 15 s in cycles 2−31), annealing (37 °C, 30 s), and elongation steps (60 °C, 30 s). Following primer extension, the samples were ethanol precipitated and resuspended in formamide loading buffer containing a 5-fold molar excess of an oligonucleotide complementary to the PNA used (Nielsen et al., 1991). Samples were resolved using 10% denaturing polyacrylamide gel electrophoresis and visualized by autoradiography. Quantification was done using a Molecular Dynamics densitometer and ImageQuant software version 3.3.

Restriction Enzyme Cleavage Inhibition Assay. Since the PNA target site is flanked by two *Pst*I restriction sites in the pA8G2 plasmid, PNA binding results in inhibition of *Pst*I restriction enzyme cleavage (Nielsen et al., 1993). This approach was used as an alternative way of measuring the amount of PNA bound to its complementary DNA target. Native supercoiled or *Ssp*I-linearized pA8G2 (100 ng) was incubated with varying amounts of PNA 655 and the desired KCl concentration in 10 mM Tris-HCl and 1 mM EDTA at pH 7.6 for 1 h at 37 °C in a final volume of 10 μL. The binding reaction was quenched using a 10-fold surplus of an oligonucleotide complementary to the PNA used, followed by *Pst*I digestion to completion in a total volume of 40 μL. *Sca*I-linearized pBluescript KS^+ (100 ng) was included as an internal control for enzyme activity. Samples were analyzed using 1% agarose/TAE gels and visualized using ethidium bromide staining and UV light. Quantification was performed by densitometric scanning of photographic negatives.

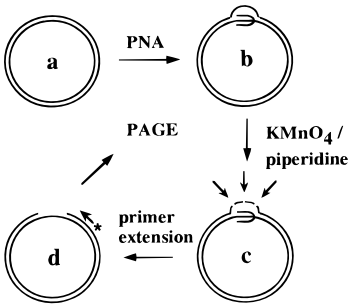

FIGURE 1: Strategy for the measurement of PNA binding to double-stranded DNA. (a) pA8G2 and PNA 575 were incubated in the desired buffer, and the resulting strand invasion complexes (b) were treated with $KMnO_4$ and cleaved with piperidine (c). Primer extension was done with a primer (arrow) 5′-labeled with ^{32}P (asterisk). The samples were resolved using polyacrylamide gel electrophoresis (PAGE) followed by autoradiography.

Topoisomer Preparation. Monomer native supercoiled DNA was incubated in the presence of 0−10 μM ethidium bromide with 5 units of wheat topoisomerase I (Promega) per microgram of DNA and incubated in 50 mM Tris-HCl (pH 7.5), 1 mM EDTA, 1 mM DTT, 20% glycerol, and 50 mM NaCl in a total volume of 50 μL for 16 h at 15 °C (or 1 h at 37 °C). The reactions were terminated by the addition of NaCl to 1 M, and the residue was extracted with 1-butanol and ethanol precipitated. The amount of nicked DNA produced was less than 5% under these conditions as estimated by scanning densitometry.

RESULTS

The experimental strategy for analyzing PNA binding to supercoiled DNA is depicted in Figure 1. PNA 575 was incubated with the pA8G2 plasmid (which contains a single complementary target), and the resulting PNA_2/dsDNA complexes (Figure 1b) were probed with permanganate. The 5,6-double bonds of thymine residues in the displaced DNA strand (resulting from PNA strand invasion) are oxidized by this treatment and are thus susceptible to alkali-catalyzed backbone cleavage (Nielsen et al., 1991, 1994b) (Figure 1c). Cleavage sites were detected as runoff products from primer extension reactions using *Taq* DNA polymerase and a ^{32}P-labeled primer (Figure 1d). Finally, the DNA fragments were resolved using polyacrylamide sequencing gels and visualized by autoradiography.

Binding of PNA to Linear and Native Supercoiled DNA. To compare the PNA binding efficiencies to linear (i.e., relaxed) versus native supercoiled ($\sigma \approx -0.051$) pA8G2 DNA, an experiment was performed in which pA8G2 was incubated with various concentrations of PNA 575 at low salt concentrations (10 mM Tris-HCl and 1 mM EDTA at pH 7.6) for 1 h at 37 °C. Virtually no signal was seen in the absence of PNA (Figure 2, lanes 1 and 7). As the PNA concentration was increased, the intensity of the series of bands which represent PNA binding increased. Comparing the intensities of the signals for PNA strand invasion suggested that binding to native supercoiled pA8G2 was

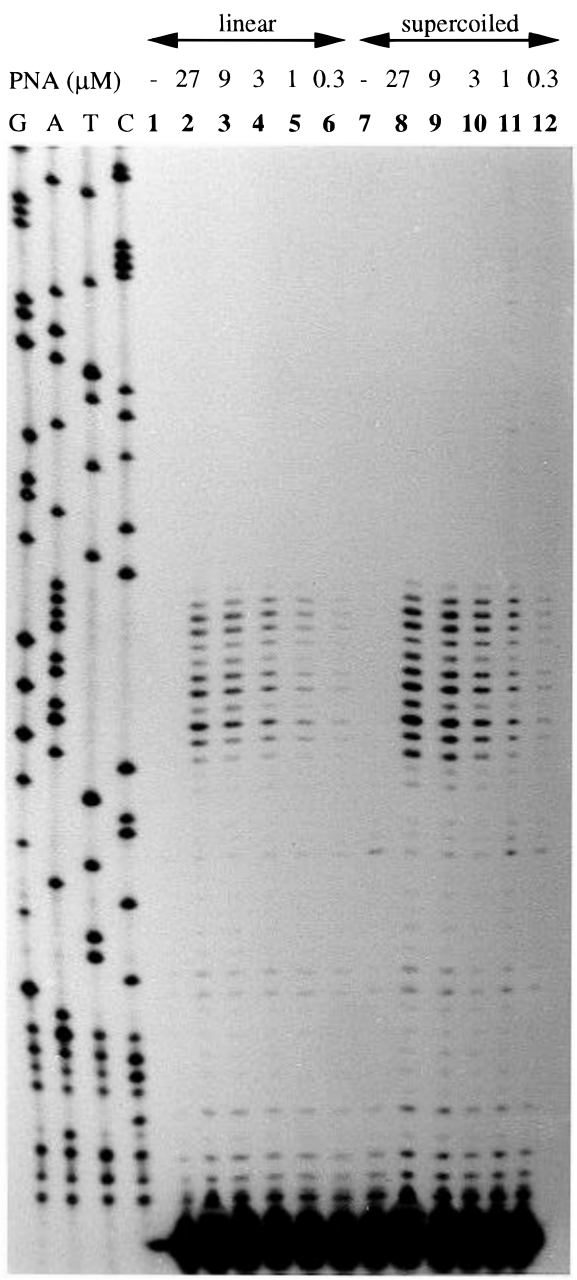

FIGURE 2: Autoradiograph showing the binding of PNA 575 to linear and native supercoiled pA8G2 DNA at low ionic strengths. Linear or native supercoiled pA8G2 was incubated with varying concentrations of PNA 575 for 1 h at 37 °C in 10 mM Tris-HCl and 1 mM EDTA at pH 7.6. PNA binding was detected by permanganate probing and primer extension. The PNA concentrations were as indicated above each lane. G, A, T, and C indicate sequence markers prepared using pA8G2 as a template and the oligonucleotide which was also used as a primer in the primer extension reactions. Note the PNA binding site (5′-$A_2GA_2GA_4$).

2−3-fold more efficient than binding to linear pA8G2. Using a restriction enzyme inhibition-based assay (see Materials and Methods) and PNA 655, this result was confirmed (data not shown).

Since the stability of the PNA_2/dsDNA complex is so high that there is no significant off rate during the experiment (Griffith et al., 1995), binding is fully kinetically controlled (Demidov et al., 1995) and thus traditional equilibrium constants are not meaningful. Consequently, all binding data are given as efficiencies which relate directly to the PNA binding rate.

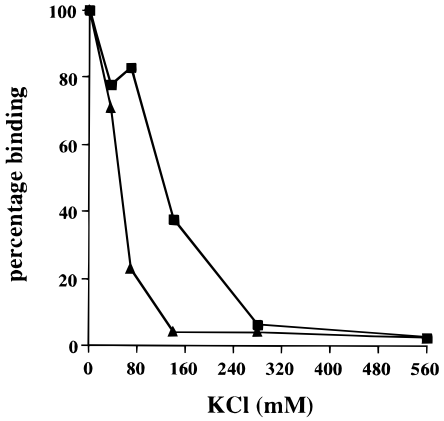

FIGURE 3: Influence of the KCl concentration on PNA strand invasion. Percentage of PNA_2/dsDNA complexes formed as a function of the KCl concentration. Linear or native supercoiled pA8G2 were incubated at 37 °C for 1 h in the presence of 5 μM PNA 575 and varying concentrations of KCl. PNA binding was determined by permanganate probing and primer extension. Quantification was done using scanning densitometric analysis of an autoradiograph similar to the one shown in Figure 2. Triangles (▲) and squares (■) denote linear and native supercoiled pA8G2, respectively.

In order to compare the effect of increasing ionic strength on the binding of PNA to linear and native supercoiled pA8G2 plasmid, various KCl concentrations were employed. The data were quantified using scanning densitometry using the signal for complete binding of PNA 575 to linear and native supercoiled pA8G2 in a low-ionic strength buffer (10 mM Tris-HCl and 1 mM EDTA at pH 7.6) as a reference (Figure 3). As the salt concentration was increased, PNA binding decreased. Notably, at 140 mM KCl (5 μM PNA 575, 37 °C, 1 h of incubation), ~45% binding was observed to native supercoiled pA8G2, whereas less than 5% binding occurred to linear pA8G2. Increasing the salt concentration further resulted in a gradual decline of PNA binding to native supercoiled DNA, and no signal was obtained at concentrations above 280 mM KCl.

One critical feature relevant to the possible future use of PNAs as antigene agents in a cellular context is the concentration necessary to obtain binding under physiological ionic strength conditions. To address this question, different PNA 575 concentrations were used for binding to linear and native supercoiled pA8G2 DNA in 140 mM KCl. Figure 4 shows the quantified data of the relative amount of PNA_2/dsDNA complex formed as a function of the PNA concentration. Saturation of PNA 575 binding to native supercoiled pA8G2 was observed around 0.6 μM PNA 575, whereas the signal for binding to linear DNA increased, at least up to 50 μM PNA 575. An analogous experiment was performed using PNA_2/dsDNA complex-mediated restriction enzyme inhibition for monitoring PNA binding to its complementary target. Linear and native supercoiled pA8G2 were incubated in the presence of varying concentrations of PNA 655 in 140 mM KCl, followed by *Pst*I restriction enzyme digestion. The quantified results are included in Figure 4. The binding efficiency of PNA 655 is slightly lower than that of PNA 575, and this we ascribe to the presence of one more positive charge in PNA 575. In both cases, however, binding to native supercoiled pA8G2 is similarly superior to the binding to linear DNA.

To investigate the PNA association rate on linear and native supercoiled templates, the time course of binding was followed in 140 mM KCl. The PNA concentrations were 1

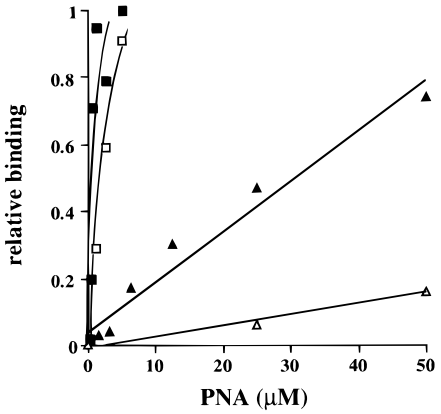

FIGURE 4: PNA concentration necessary to obtain strand invasion in 140 mM KCl. The relative amount of PNA_2/dsDNA complex formed as a function of the PNA concentration. PNA 575 at varying concentrations was incubated with linear or native supercoiled pA8G2 for 1 h at 37 °C in the presence of 140 mM KCl and analyzed using permanganate probing and primer extension. Quantification was done as in Figure 3. PNA 655 was incubated with 100 ng of linear or supercoiled pA8G2 in the presence of 140 mM KCl for 1 h at 37 °C, followed by complete *Pst*I digestion, 1% agarose/TAE gel electrophoresis (1.2 V cm^{-1}, 16 h), and visualization using ethidium bromide staining. Photographic negatives were used for quantification by scanning densitometry. Closed symbols represent PNA 575, and open symbols represent PNA 655. Triangles (▲/△) and squares (■/□) denote linear and native supercoiled pA8G2, respectively.

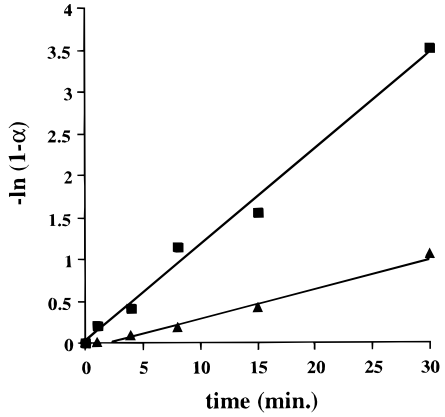

FIGURE 5: Kinetics of PNA strand invasion in 140 mM KCl. Plot of $-\ln(1-\alpha)$ as a function of the time of incubation (α indicates the fraction of PNA_2/dsDNA complexes formed). Linear or native supercoiled pA8G2 was incubated with 1 or 40 μM PNA 575, respectively, for various periods of time at 37 °C in the presence of 140 mM KCl. Quantification was done as in Figure 3. Triangles (▲) and squares (■) denote linear and native supercoiled pA8G2, respectively.

and 40 μM with native supercoiled and linear pA8G2, respectively. Presenting the quantified data in a plot of $-\ln(1-\alpha)$ (where α is the fraction of PNA_2/dsDNA complex) as a function of time yielded the pseudo-first-order association rate constants (Demidov et al., 1995) $k_{\psi lin} = 0.04$ min^{-1} and $k_{\psi sc} = 0.1$ min^{-1} for binding to linear and native supercoiled pA8G2, respectively (Figure 5). Assuming that the rate constants exhibit equal dependence on the PNA concentration, a rate ratio of 210 can be deduced.[2] In analogous experiments performed using identical PNA concentrations (10 μM), mean rate constants of $k_{\psi lin} = 0.01 \pm 0.003$ min^{-1} and $k_{\psi sc} = 1.9 \pm 0.6$ min^{-1} were obtained (plotted in Figure 7b), yielding a mean rate ratio of 190.

The influence of a polyvalent cation on PNA binding to linear and native supercoiled pA8G2 was examined using various concentrations of spermidine in the binding reaction. The quantified data were plotted as the percentage of PNA_2/dsDNA complex formed as a function of the spermidine concentration (Figure 6), this indicated that PNA binding to linear pA8G2 is reduced to less than 5% in the presence of 2−3 mM spermidine, whereas ~30% PNA_2/dsDNA complex was formed with native supercoiled pA8G2 even at 9 mM spermidine.

Similarly, we find that $MgCl_2$ has no measureble effect on the binding of PNA 575 to native supercoilied pA8G2 up to 27 mM, whereas the binding to linear pA8G2 is completely inhibited at this concentration (data not shown).

Thus, the inhibitory effect of salts on PNA binding ranks $spermidine^{3+} > Mg^{2+} > K^+$ which mirrors the effect of these cations on DNA thermal stability.

Topoisomer Analysis. The relationship between the rate of PNA binding and DNA superhelical density in 140 mM KCl was established by using pA8G2 topoisomer populations

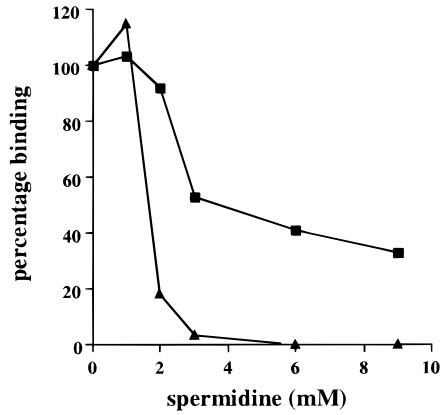

FIGURE 6: Influence of spermidine on PNA strand invasion. Percentage of PNA_2/dsDNA complexes formed as a function of the spermidine concentration. Linear or native supercoiled pA8G2 was incubated with spermidine (pH 7) and 5 μM PNA 575 for 1 h at 37 °C. Quantification was done as in Figure 3. Triangles (▲) and squares (■) denote linear and native supercoiled pA8G2, respectively. The apparent transient increase in PNA binding at low spermidine concentrations is ascribed to experimental inaccuracy.

harboring different levels of mean superhelical density (σ) (Figure 7a). The pseudo-first-order association rate constants were obtained from the tangent to the initial rate of PNA_2/dsDNA complex formation. The PNA binding exhibits a dramatic dependence on superhelical density, and from the plot of $k_\psi(\sigma)$ versus $-\sigma$, it is seen that the results fit an exponential relationship (Figure 7b), $k_\psi(\sigma) = k_{\psi lin} e^{-\sigma\delta}$, where δ is a constant of 105.

Activation Energy for PNA Binding. The activation energy [$Ea(\sigma)$] for PNA strand invasion binding to linear and native supercoiled pA8G2 was estimated by measuring the temperature dependence for the association in 140 mM KCl. The Arrhenius plots [$\ln k_\psi(\sigma)$ versus $1/T$] yield activation energies of $Ea_{lin} \approx 93$ kJ mol^{-1} and $Ea_{sc} \approx 48$ kJ mol^{-1} for binding to linear and native supercoiled pA8G2, respectively (Figure 8). Not surprisingly, the activation energy is considerably lower (45 kJ mol^{-1}) for PNA binding to supercoiled pA8G2.

[2] The ratio for PNA binding to native supercoiled and linear pA8G2 was obtained according to the expression $(k_{\psi sc}/k_{\psi lin})(40^\gamma/1^\gamma)$, where $\gamma = 1.2$ [experiments not shown; cf. Demidov et al. (1995)].

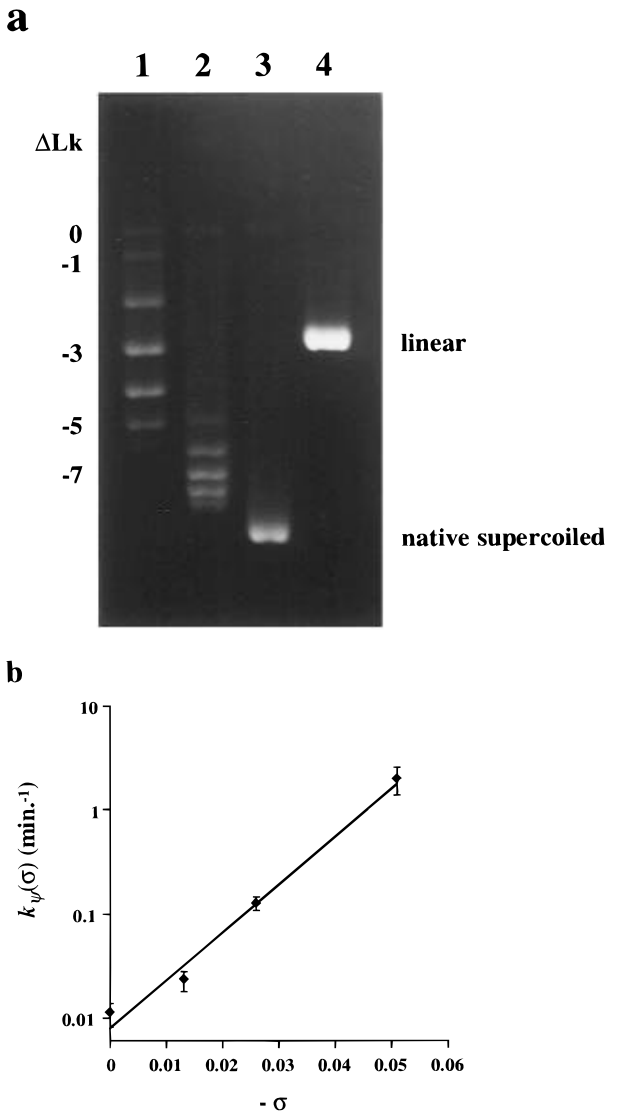

FIGURE 7: Influence of the superhelical density on PNA strand invasion. The rate constants, $k_\psi(\sigma)$ (min^{-1}), for PNA 575 binding to pA8G2 topoisomer populations with different mean superhelical densities were determined in 140 mM KCl using the permanganate probing and primer extension assay. (a) Agarose (1%/TAE) gel electrophoretic analysis of pA8G2 topoisomers generated by incubating native supercoiled pA8G2 with topoisomerase I in the presence of 2 μM (lane 1) or 3 μM (lane 2) ethidium bromide. The mean superhelical densities of the populations were determined using scanning densitometric analysis of photographic negatives. This yielded $\sigma = -0.013$ (lane 1), $\sigma = -0.026$ (lane 2), and $\sigma \approx -0.051$ (lane 3 and experiments not shown). Lane 4 is linear pA8G2. (b) Semilogarithmic plot of $k_\psi(\sigma)$ (min^{-1}) versus $-\sigma$. PNA 575 (10 μM) was incubated with the pA8G2 topoisomers shown in panel a for various periods of time at 37 °C in the presence of 140 mM KCl. Quantification was done using scanning densitometric analysis of autoradiographs similar to the one shown in Figure 2. The pseudo-first-order rate constants were obtained from the tangent to the initial rates of PNA strand invasion in plots of $-\ln(1-\alpha)$ versus time (see Figure 5). Error bars indicate standard error of the mean (of three to four experiments).

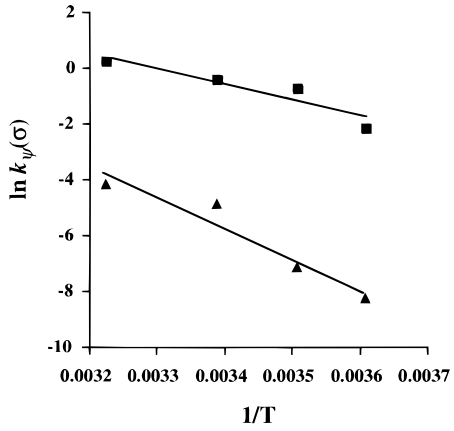

FIGURE 8: Arrhenius plot for determination of the activation energy for PNA strand invasion. The influence of the temperature on the rate of PNA strand invasion was determined using permanganate probing and primer extension. Linear or native supercoiled pA8G2 was incubated at 4, 12, 22, or 37 °C, with 10 μM PNA 575 for various periods of time in the presence of 140 mM KCl. Permanganate probing was done by diluting each sample 10-fold at 0 °C in a solution containing 0.3 M KCl and 1 mM $KMnO_4$. The reactions were stopped after 1 min. The pseudo-first-order rate constants were obtained from the tangent to the initial rates of PNA strand invasion in plots of $-\ln(1-\alpha)$ versus time (see Figure 5). The (negative) slope in the plot of ln $k_\psi(\sigma)$ versus $1/T$ (Kelvin) multiplied by the gas constant, R, yielded the activation energies of $Ea_{lin} \approx 93$ kJ mol^{-1} and $Ea_{sc} \approx 48$ kJ mol^{-1} for PNA binding to linear and native supercoiled pA8G2, respectively. Triangles (▲) and squares (■) denote linear and native supercoiled pA8G2, respectively.

DISCUSSION

The present results clearly show that PNA binds more efficiently to supercoiled DNA than to linear (relaxed) DNA and that this difference is especially pronounced (2 orders of magnitude) at elevated ionic strengths and notably also at physiological ionic strengths (140 mM KCl). The results also reveal an exponential dependence of the binding rate on the DNA (negative) superhelical density (σ). In addition, spermidine (and $MgCl_2$) has a detrimental effect on PNA binding which is qualitatively similar to the effect of KCl such that PNA binding tolerates higher polycation concentrations with native supercoiled DNA than with linear DNA.

These results have implications for the prospects of using PNA as an antigene reagent *in vivo* as well as for the dynamics of supercoiled DNA and may therefore also be relevant for the discussion of the effect of supercoiling on enzyme recognition. In addition, the results suggest novel applications of PNA as a molecular biology tool.

The pronounced inhibitory effect of moderate salt concentrations on the binding of PNA to double-stranded DNA has raised concerns about the prospect of using PNA as an antigene reagent (Nielsen et al., 1994a,b; Peffer et al., 1993). However, development of bis-PNAs (Egholm et al., 1995) (especially positively charged bis-PNAs) was a significant improvement since these were recently shown to bind double-stranded DNA at close to physiological ionic strengths, although with slow association kinetics (Griffith et al., 1995; P. E. Nielsen, unpublished experiments).

Our results suggest that PNA strand invasion inside a cell may be much more efficient than previously anticipated since DNA *in vivo* is predominantly negatively supercoiled. For instance, the superhelical density of the *E. coli* nucleoid DNA was measured as $\sigma \approx -0.05$ (Sinden et al., 1980), although part of this is probably restrained *in vivo*. Furthermore, in the supercoil twin domain model by Liu and Wang (1987), elongating polymerases are proposed to induce negative supercoils upstream (and positive supercoils downstream) of the transcription elongation complex. Several studies using plasmid DNA *in vitro* (Tsao et al., 1989) or various cellular systems (Wu et al., 1988; Giaever & Wang, 1989; Dunaway & Ostrander, 1993; Bowater et al., 1994a) support this basic model [reviewed by Wang and Lynch (1993)].

Although the global level of unrestrained supercoiling in eukaryotes is near zero [see, e.g., Sinden et al. (1980)], localized negative tension has been demonstrated in association with transcriptionally active genomic DNA (Ljungman & Hanawalt, 1995; Jupe et al., 1993). Thus, it is reasonable to expect that negative supercoiling will greatly facilitate PNA binding to double-stranded DNA of transcriptionally active genes *in vivo*. This view is strengthened by the observation that transcription *per se* of linear DNA, probably through PNA capture of the transcription bubble, facilitates PNA binding to double-stranded DNA (Larsen & Nielsen, 1996).

The present model for strand displacement binding of PNA involves DNA base pair "breathing" [defined as the transient (lateral) opening of a base pair] as a crucial and, at least partially, rate-limiting step in the process. Thus, an increase in the PNA binding rate could be due to increased base pair breathing. Alternatively, formation of persistent open structures (e.g., cruciforms and H-DNA) could account for faster PNA strand invasion kinetics with negatively supercoiled DNA than with relaxed DNA. However, we see no evidence for such persistent open structures in the pA8G2 plasmid in general and proximal to the PNA target in particular. First, two-dimensional gel electrophoresis did not reveal structural transitions in the range of superhelicities examined (experiments not shown). Second, permanganate sensitivity was equally low with linear and native supercoiled DNA in the absence of PNA. Third, the sequence does not indicate any propensity for structural transitions, and fourth, large-scale openings are suppressed by low concentrations of salt at even high levels of superhelical density (Bowater et al., 1994b).

In a very simplified model, the Watson−Crick PNA/dsDNA duplex strand invasion complex has been considered a key (albeit unstable) intermediate in the binding process (Demidov et al., 1995). It is clear that the thermodynamic equilibrium constant for the formation of such a complex can be influenced by supercoiling in two ways. An increase in DNA breathing would increase the on rate, while the off rate will be reduced since binding relieves superhelical turns in the DNA. The differential salt effect on PNA binding to relaxed versus supercoiled DNA (e.g., Figure 3) may relate to these two rate constants. Since the helical repeat (and as a consequence σ) has been found to be virtually unaffected (Taylor & Hagerman, 1990) or only slightly influenced by these ionic conditions (Anderson & Bauer, 1978), the PNA off rate should not change significantly either.[3] Therefore, the differential salt effect is most likely caused by a change in the on rate and thus in DNA breathing. This leads us to propose that breathing in supercoiled DNA as opposed to relaxed DNA [as exemplified by oligonucleotide duplexes (Braunlin & Bloomfield, 1988)] is very ionic strength dependent, being more pronounced at higher ionic strengths. The results suggest that supercoiled DNA ($\sigma \approx -0.051$) is 2 orders of magnitude more dynamic at physiological ionic strengths than DNA free of topological constraints. We also note that theoretical considerations have brought Vologodskii et al. (1979) to conclude that supercoiling enhances DNA breathing. This is, of course, biologically relevant since several enzymatic actions on double-stranded DNA, such as nucleobase methylation (Klimasauskas et al., 1994) and transcription initiation (*vide infra*), are likely to be influenced by if not to rely on DNA breathing.

Since the breathing dynamics could be closely related to the activation energy for the structural change necessary for PNA strand invasion, it was relevant to compare the activation energies [Ea(σ)] for PNA binding to linear versus supercoiled DNA. As could be expected from the difference in PNA binding rates, the activation energy for PNA binding to linear DNA is significantly higher ($\sim$45 kJ mol^{-1}) than for PNA binding to native supercoiled DNA, and reassuringly, the measured difference in binding rate of approximately 200 translates to a theoretical difference in activation energy of $\sim$47 kJ mol^{-1}.

We ascribe the major part of the activation energy of PNA binding to the transient opening (breathing) of the DNA helix at the PNA target which is required for initial strand invasion. It is not known at present how many base pairs are involved in the nucleation, but the activation energy for opening of one base pair as measured by NMR is approximately 80 kJ mol^{-1} (Kochoyan et al., 1990); the activation energy for complete melting of an octanucleotide (Braunlin & Bloomfield, 1991) or a heptanucleotide duplex (Pardi & Tinoco, 1982) was measured as $\sim$200 kJ mol^{-1}. Therefore, the results would be consistent with opening of only a few base pairs as a rate-limiting step in PNA binding.

It is important to emphasize that the present model for PNA binding most certainly is an oversimplified one since the overall PNA binding reaction involves association and dissociation rate constants for at least 40 nucleobase interactions. In addition, binding of each nucleobase is presumably dependent on the interactions made by the neighboring nucleobases thereby providing added complexity.

Computations have shown that bending of the DNA helix reduces the opening energy (and thus probably also the opening activation energy) by a factor of 4 at a bending corresponding to a 15 Å radius of curvature (Ramstein & Lavery, 1988). A similar effect could be responsible for the decreased activation energy observed here upon PNA binding to supercoiled DNA, since DNA is bent by supercoiling. However, the average bend angle for native supercoiled pA8G2 corresponds to a 115 Å radius of curvature [assuming the number of supercoils = 0.9ΔLk (Boles et al., 1990), and a 3.4 Å helical rise per base pair], and thus, bending alone most likely does not account for the observed increase in PNA binding to negatively supercoiled DNA.

It is now well-established that transcription from a variety of prokaryotic and eukaryotic promoters is strongly affected by DNA supercoiling (Borowiec & Gralla, 1987; Bowater et al., 1994a; Dunaway & Ostrander, 1993; Harland et al., 1983; Mizutani et al., 1991; Parvin & Sharp, 1993; Schultz et al., 1992; Weintraub et al., 1986), and the level of DNA supercoiling is therefore one of the parameters that cells may exploit in transcriptional gene regulation. The present results may be relevant for this discussion. In the model of Buc and McClure (1985), transcriptional activation by *E. coli* RNA polymerase is divided into three kinetically defined steps:

$$R + P \overset{k_1}{\rightleftharpoons} RP_c \overset{k_2}{\rightleftharpoons} RP_i \overset{k_3}{\rightleftharpoons} RP_o$$

(R = RNA polymerase, P = promoter, RP_c = closed complex, and RP_i = intermediate complex, RP_o = open

[3] From the results of Anderson and Bauer (1978), a change in $-\sigma$ from 0.051 to 0.054 when going from 0 to 140 mM KCl can be expected. This corresponds to an increase in $k_\psi(\sigma)$ from 2.0 to 2.8 according to the relationship $k_\psi(\sigma) = k_{\psi \mathrm{lin}} e^{-\sigma\delta}$.

complex). k_1 is the rate constant for initial binding of the RNA polymerase to the promotor DNA, and k_2 and k_3 are the rate constants attributed to a conformational change in the RNA polymerase (k_2) prior to DNA unstacking and melting (k_3). Viewing PNA strand invasion binding as a primitive model for the RP_i-RP_o transition suggests two implications for transcription initiation. First, DNA melting in the initiation complex may be a consequence of DNA dynamics rather than being induced by RNA polymerase itself (i.e., the enzyme function as a trap for DNA strand dissociation). Second, since the PNA analogy suggests that k_3 has an exponential dependence on the superhelical density, the decline in transcription initiation rate seen with some promotors above an optimum level of negative superhelicity (Borowiec & Gralla, 1987) may be attributed exclusively to a decrease in k_1 (i.e., the DNA structure is less favored for initial recognition by RNA polymerase at a high superhelical density).

In conclusion, we have shown that PNA binding to double-stranded DNA at physiologically relevant ionic strength conditions is dramatically influenced by the superhelical density of DNA. This result significantly reduces the reservations previously raised concerning the predicted inefficient binding of PNA to double-stranded DNA *in vivo*. Furthermore, the results suggest that the base pair breathing dynamics at physiological ionic strengths is highly increased with negative superhelix density, and this may in part explain the rate enhancement observed for some promoters with supercoiled DNA templates. Finally, the results invite the use of PNA binding as a quantitative, *in situ* probe for (localized) DNA supercoiling, and thus for the identification and characterization of active genes. This could complement the use of psoralen for monitoring DNA superhelicity (Sinden et al., 1980; Jupe et al., 1993; Ljungman & Hanawalt, 1995).

ACKNOWLEDGMENT

We thank Dr. Hans Jakob Larsen for discussions and comments on the manuscript.

REFERENCES

Anderson, P., & Bauer, W. (1978) *Biochemistry 17*, 594−601.

Boles, T. C., White, J. H., & Cozzarelli, N. R. (1990) *J. Mol. Biol. 213*, 931−951.

Borowiec, J. A., & Gralla, J. D. (1987) *J. Mol. Biol. 195*, 89−97.

Bowater, R., Aboul, E. F., & Lilley, D. M. (1992) *Methods Enzymol. 212*, 105−120.

Bowater, R. P., Chen, D., & Lilley, D. M. (1994a) *Biochemistry 33*, 9266−9275.

Bowater, R. P., Aboul, E. F., & Lilley, D. M. (1994b) *Nucleic Acids Res.* 22, 2042−2050.

Braunlin, W. H., & Bloomfield, V. A. (1988) *Biochemistry 27*, 1184−1191.

Braunlin, W. H., & Bloomfield, V. A. (1991) *Biochemistry 30*, 754−758.

Buc, H., & McClure, W. (1985) *Biochemistry 24*, 2712−2723.

Cherny, D. Y., Berlotserkovskii, B. P., Frank-Kamenetskii, M. D., Egholm, M., Buchardt, O., Berg, R. H., & Nielsen, P. E. (1993) *Proc. Natl. Acad. Sci. U.S.A. 90*, 1667−1670.

Christensen, L., Fitzpatrick, R., Gildea, B., Petersen, K., Hansen, H. F., Koch, T., Egholm, M., Buchardt, O., Nielsen, P. E., Coull, J., & Berg, R. (1995) *J. Pept. Sci. 3*, 175−183.

Demidov, V., Frank-Kamenetskii, M. D., Egholm, M., Buchardt, O., & Nielsen, P. E. (1993) *Nucleic Acids Res. 21*, 2103−2107.

Demidov, V. V., Cherny, D. I., Kurakin, A. V., Yavnilovich, M. V., Malkov, V. A., Frank-Kamenetskii, M. D., Sönnichsen, S., & Nielsen, P. E. (1994) *Nucleic Acids Res. 22*, 5218−5222.

Demidov, V. V., Yavnilowich, M. V., Berlotserkovskii, B. P., Frank-Kamenetskii, M. D., & Nielsen, P. E. (1995) *Proc. Natl. Acad. Sci. U.S.A. 92*, 2637−2641.

Dunaway, M., & Ostrander, E. A. (1993) *Nature 361*, 746−748.

Egholm, M., Christensen, L., Dueholm, K. L., Buchardt, O., Coull, J., & Nielsen, P. E (1995) *Nucleic Acids Res. 23*, 217−222.

Giaever, G. N., & Wang, J. C. (1988) *Cell 55*, 849−856.

Griffith, M. C., Risen, L. M., Greig, M. J., Lesnik, E. A., Sprankle, K. G., Griffey, R. H., Kiely, J. S., & Freier, S. M. (1995) *J. Am. Chem. Soc. 117*, 831−832.

Hanvey, J. C., Peffer, N. J., Bisi, J. E., Thomson, S. A., Cadilla, R., Josey, J. A., Ricca, D. J., Hassman, C. F., Bonham, M. A., Au, K. G., Carter, S. G., Bruckenstein, D. A., Boyd, A. L., Noble, S. A., & Babiss, L. E. (1992) *Science 258*, 1481−1485.

Harland, R. M., Weintraub, H., & McKnight, S. L. (1983) *Nature 302*, 38−43.

Hélène, C. (1991) *Anti-Cancer Drug Des. 6*, 569−584.

Jupe, E. R., Sinden, R. R., & Cartwright, I. L. (1993) *EMBO J. 12*, 1067−1075.

Klimasauskas, S., Kumar, S., Roberst, R. J., & Cheng, X. (1994) *Cell 76*, 357−369.

Kochoyan, M., Leroy, J. L., & Guéron, M. (1990) *Biochemistry 29*, 4799−4805.

Larsen, H. J., & Nielsen, P. E. (1996) *Nucleic Acids Res. 24*, 458−463.

Liu, L. F., & Wang, J. C. (1987) *Proc. Natl. Acad. Sci. U.S.A. 84*, 7024−7027.

Ljungman, M., & Hanawalt, P. C. (1995) *Nucleic Acids Res. 23*, 1782−1789.

Maher, L. J., III (1992) *BioEssays 14*, 807−815.

Mizutani, M., Ohta, T., Watanabe, H., Handa, H., & Hirose, S. (1991) *Proc. Natl. Acad. Sci. U.S.A. 88*, 718−722.

Nielsen, P. E., Egholm, M., Berg, R. H., & Buchardt, O. (1991) *Science 254*, 1497−1500.

Nielsen, P. E., Egholm, M., Berg, R. H., & Buchardt, O. (1993) *Nucleic Acids Res. 21*, 197−200.

Nielsen, P. E., Egholm, M., & Buchardt, O. (1994a) *Gene 149*, 139−145.

Nielsen, P. E., Egholm, M., & Buchardt, O. (1994b) *J. Mol. Recognit. 7*, 165−170.

Ørum, H., Nielsen, P. E., Egholm, M., Berg, R. H., Buchardt, O., & Stanley, C. (1993) *Nucleic Acids Res. 21*, 5332−5336.

Pardi, A., & Tinoco, I., Jr. (1982) *Proc. Natl. Acad. Sci. U.S.A. 21*, 4686−4693.

Parvin, J. D., & Sharp, P. A (1993) *Cell 73*, 533−540.

Peffer, N. J., Hanvey, J. C., Bisi, J. E., Thomson, S. A., Hassman, C. F., Noble, S. A., & Babiss, L. E. (1993) *Proc. Natl. Acad. Sci. U.S.A. 90*, 10648−10652.

Ramstein, J., & Lavery, R. (1988) *Proc. Natl. Acad. Sci. U.S.A. 85*, 7231−7235.

Sambrook, J., Fritsch, E. F., & Maniatis, T. (1989) in *Molecular Cloning: A Laboratory Manual* (Nolan, C., Ed.) Cold Spring Harbor Laboratory Press, Plainview, NY.

Schultz, M. C., Brill, S. J., Ju, Q., Sternglanz, R., & Reeder, R. H. (1992) *Genes Dev. 6*, 1332−1341.

Sinden, R. R., Carlson, J. O., & Pettijohn, D. E. (1980) *Cell 21*, 773−783.

Taylor, W. H., & Hagerman, P. J. (1990) *J. Mol. Biol. 212*, 363−376.

Tsao, Y. P., Wu, H. Y., & Liu, L. F. (1989) *Cell 56*, 111−118.

Vologodskii, A. V., & Cozzarelli, N. R. (1994) *Annu. Rev. Biophys. Biomol. Struct. 23*, 609−643.

Vologodskii, A. V., Lukashin, A. V., Anshelevich, V. V., & Frank-Kamenetskii, M. D. (1979) *Nucleic Acids Res. 6*, 967−982.

Wang, J. C. (1979) *Proc. Natl. Acad. Sci. U.S.A. 76*, 200−203.

Wang, J. C., & Lynch, A. S. (1993) *Curr. Opin. Gen. Dev. 3*, 764−768.

Weintraub, H., Cheng, P. F., & Conrad, K. (1986) *Cell 46*, 115−122.

Wu, H. Y., Shy, S. H., Wang, J. C., & Liu, L. F. (1988) *Cell 53*, 433−440.

BI960436K